

Pulsed generation of electronic-vibrational quantum coherences and non-classicality in chemical and biophysical systems

N. F. Johnson,¹ F. J. Gómez-Ruiz,² O. L. Acevedo,³ F. J. Rodríguez,² and L. Quiroga²

¹*Department of Physics, University of Miami, Coral Gables, FL 33124, U.S.A.*

²*Departamento de Física, Universidad de los Andes, A.A. 4976, Bogotá D. C., Colombia*

³*JILA, University of Colorado, Boulder, CO 80309, U.S.A.*

(Dated: September 3, 2022)

A fundamental question has arisen as to why robust coherences have been observed in so many driven chemical and biophysical systems containing large numbers of components (e.g. dimers), and whether these coherences can be truly quantum mechanical. Because of these systems' inherent many-body complexity, theoretical treatments to date have made approximations such as limiting the number N of system components (e.g. one dimer $N = 1$), truncating non-Markovian effects, and treating aspects of the system as stochastic or averaged. Here we avoid these assumptions by analyzing the exact real-time evolution of a driven, generic out-of-equilibrium vibrational-electronic system that comprises an arbitrary number of components (e.g. dimers) N . Our results predict that a new form of dynamically-driven quantum coherence can arise surprisingly easily for general N and without having to access the empirically challenging strong-coupling regime. The resulting electronic-vibrational entanglement is driven by the *speed* of changes in the internal dynamics, and is accompanied by distinct yet complementary non-classicalities within each subsystem that have eluded previous analyses. Our findings show robustness to losses and noise, and have functional implications at the systems level for a wide range of chemical, biophysical and also physical systems.

The recent landmark *Nature* review of Scholes et al. [1] points to the surprising ubiquity of coherence phenomena across chemical and biophysical systems that are driven from the outside – typically by some high-power light source which generates vibrational responses on the ultrafast scale [1–43]. It is suspected that many of these coherence phenomena involve some generic form of quantum mechanical interference between the many-body wave function amplitudes of the system's electronic and vibrational components [1–3, 6, 12]. In addition, the body of evidence [1–43] suggests that coherence phenomena in chemical and biophysical systems of general size can show a surprising level of robustness and extended survival time in the presence of noise. Reference [1] also suggests that these observations are so ubiquitous that focus should be turned toward exploring the connection between coherence and possible biological function. Unfortunately, it is impossible to evaluate the exact quantum evolution of a driven mixed exciton-carrier-vibrational system of arbitrary size. Any theoretical analysis will therefore, by necessity, make approximations in terms of the choice of specific simplifying geometries, the specific number of system components included in the calculation (e.g. $N = 1$ dimer as in Ref. [6]), choices about the coupling between the various excitations of the system, and the manner in which memory effects are averaged over or truncated. While convenient computationally, such approximations have left open the question of the fundamental nature of such coherence phenomena, and how they might possibly be generated as the number N of system components (e.g. dimers) increases towards the tens, hundreds or thousands as in real experimental samples.

Here we address this fundamental question [1]. Specifically, our calculations predict that strong quantum coherences and non-classicalities can be generated surprisingly easily in a driven chemical or biophysical system comprising a general number N of components (Fig. 1, e.g. dimers) without needing to access the strong-coupling regime, but instead as a result of its internal dynamics – in particular, the *speed* of the changes (Fig. 2). As a corollary, our findings suggest that strong quantum coherences will already have been generated in experiments to date that happen to have fallen in this broad speed regime, and hence offer a possible unified explanation of these. While not approximation-free, our theoretical approach avoids the most common approximations listed above, and yields results that in principle apply to any number of components N and include memory effects directly. The Hamiltonian that we consider is purposely simpler and more generic than many studied to date, in order that we can focus attention on understanding the conditions under which large quantum coherence and non-classicality (Fig. 3) are generated. In this way, we are also able to identify a functional advantage for such collective quantum coherence at the level of an entire system for general N .

In the following sections, we first provide a detailed justification for our approach and its general applicability. We then present our main quantitative results (Figs. 2–3) before discussing the overall robustness in the presence of noise and losses.

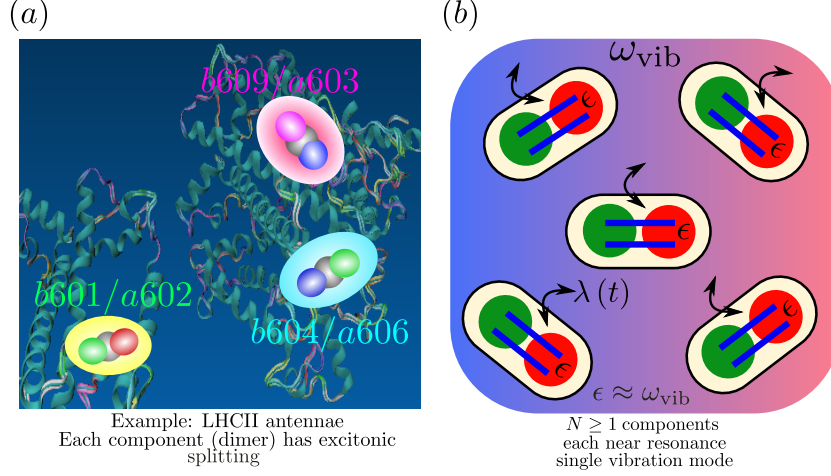


FIG. 1: (a) **Prototype dimer.** This is a representation of the LHCII antennae of *Spinacia oleracea* (Protein Data Bank ID code 1RWT [6, 44]) illustrating three types of dimer pairs, each of which comprises close Chl_b-Chl_a chlorophylls [6]. Any one of these three dimer types is a candidate component for our N -component model. (b) Schematic representation of the single mode, resonant version of our model (Eq. (2)). Each chlorophyll pair in Fig. 1(a) contains two split excitonic energy levels with separation ϵ and can be regarded as the basic two-level component in our N -component system. For example, the Chl_{b601}-Chl_{a602} pair has $\epsilon = 667.7\text{cm}^{-1}$ and $\omega_{\text{vib}} = 742.0\text{cm}^{-1}$ which means they are close in energy (i.e. $\epsilon \approx \omega_{\text{vib}}$) [6]. The coupling ($\lambda(t)$) is time-dependent in order to capture the complex swathe of additional non-equilibrium, anharmonic interactions that can be generated in the system by high-intensity pulsed light. Though the wavefunction for each level is delocalized within each pair, the wavefunction and hence probability for the lower (upper) level is more localized on the chromophore with the lower (higher) energy, hence a transition between the two represents a spatial transfer of energy from one chromophore to another [6].

FORMAL DETAILS

Driven system of arbitrary size A general chemical or biophysical system that contains an arbitrary number of components and is driven by some external perturbation beyond linear response, will have a time-dependent Hamiltonian that resembles the following schematic form:

$$H_{\text{gen}}(t) = \sum_{\{\text{vib}\}} a_{\text{vib}}^\dagger a_{\text{vib}} + \sum_{\{\text{ext-field}\}} b_{\text{ext-field}}^\dagger b_{\text{ext-field}} + \sum_{\{\text{elect}\}} c_{\text{elect}}^\dagger c_{\text{elect}} + \Lambda(\{\{a_{\text{vib}}\}, \{b_{\text{ext-field}}\}, \{c_{\text{elect}}\}\}; t) \quad (1)$$

where $\{a_{\text{vib}}\}$, $\{b_{\text{ext-field}}\}$ and $\{c_{\text{elect}}\}$ represent the set of all vibrational, externally-generated and electronic modes respectively, i.e. $\{a_{\text{vib}}\}$ includes all delocalized (phonons) and localized (vibrational) modes, $\{b_{\text{ext-field}}\}$ includes the quantization of the external field which may, for example, be photonic but is not necessarily black-body or weak. The operators $\{c_{\text{elect}}\}$ account for every electron and hence hole excitation, including those that form excitons, and therefore when the interaction $\Lambda(\dots)$ is included, they can describe any exciton as well as free carriers, and any coupling between them. Our implementation of Eq. (1) accounts for an arbitrary number N of molecular components (e.g. N identical dimers from Fig. 1) whose excitonic levels become coupled to particular vibrational modes of the system, as in Fig. 1(b). The coupling between the electronic and vibrational components is enhanced by dynamical fields that can be created inside the system as a result of a strong external driving field (e.g. pulsed light). Since we are interested in nonlinear measurement techniques in which out-of-equilibrium effects arise, this induced dynamical coupling arises from the anharmonic interactions that tend to cycle in time as the molecular system distorts in response to periodic perturbations.

Our approach makes the reasonable assumption that the driven system with anharmonic interactions can be described phenomenologically using classical fields instead of full quantum field operators. This has the effect of averaging over some higher-order quantum fluctuations while including others rather precisely. Specifically, we replace quadratic operator terms by a c -number with a time-dependent coefficient which acts as an effective pump on the remaining excitations. Reference [45] further demonstrates the reasonability of this approximation for the explicit case of control of non-Markovian effects in the dynamics of polaritons generated in semiconductor microcavities at high laser-pumping pulse intensities – however the same approach can be applied to any other Hamiltonian of the general form of Eq. (1). The section ‘Temporal memory from driving field’ provides the detailed justification. As a result, an effective classical intensity sets the coupling strength which becomes time-dependent. The resulting Hamiltonian can be written as that

describing a time-dependent generalized Dicke-like model for any $N \geq 1$ [46]:

$$H_N(t) = \sum_{\beta} \omega_{\beta} a_{\beta}^{\dagger} a_{\beta} + \sum_{i=1}^N \sum_{\alpha_i \in i} \frac{\epsilon_{\alpha_i}}{2} \sigma_{z, \alpha_i}^i + \sum_{\beta} \sum_{i=1}^N \sum_{\alpha_i \in i} \frac{\lambda_{\alpha_i, \beta}^i(t)}{\sqrt{N}} (a_{\beta}^{\dagger} + a_{\beta}) \sigma_{x, \alpha_i}^i \quad (2)$$

where σ_{p, α_i}^i denotes the Pauli operators for excitation α_i on molecular component (e.g. dimer, Fig. 1(b)) i with $p = x, z$. The first term is the set of vibrational modes $\{\beta\}$ which may or may not be localized around certain locations. The second term represents the electronic excitations $\{\alpha_i\}$ localized on each of the components $i = 1, \dots, N$ (e.g. dimers, Fig. 1(b)). The two electronic states on each component may be hybrid excitonic states, e.g. $|X\rangle$ and $|Y\rangle$ in Ref. [6]. The third term gives the coupling between the electronic and vibrational terms, by means of which energy and quantum coherence can be transferred back and forth between these molecular components $\{\alpha_i\}$ and the vibrational modes $\{\beta\}$. We stress that our choice of N components in Eq. (2) does not mean that this is necessarily the total number of molecular units in the system under study: It may happen that in practice only some portion of the macromolecular system is probed by the experiment, hence N can in principle be tailored to account for this.

Equation (2) is quite general in terms of its scalability to any number of components, and can serve a similar function to models such as the Ising model in getting at the general universality of behaviors to be expected across materials [46]. This is important given the wide range of chemically diverse systems in which generic coherence effects are observed [1–43] which in turn motivates our generic as opposed to material-specific approach. We have already shown that for variants of Eq. (2) there is a universal dynamical scaling behavior for a particular class concerning their near-adiabatic behavior, in particular the Transverse-Field Ising model, the Dicke Model and the Lipkin-Meshkov-Glick model [46]. Since the entire system is for the moment considered closed, there is no overall dissipation but it does allow for the fact that the molecular subsystem components may be losing energy to the vibrational subsystem and vice versa. It also makes no assumptions about the memory in either the molecular dynamics or the vibration system, or their coupling. Specifically, it is non-Markovian by design; it includes all memory effects; it is valid irrespective of how fast or slow $\lambda_{\alpha_i, \beta}^i(t)$ varies or its temporal profile; it applies irrespective of the individual spectra at each site of the spectrum of vibrational modes; and most importantly, it applies to any value of N . If we consider the limiting case of just $N = 1$ dimer *and* we further assume there is no time-dependence in the coupling term λ (both of which are strong and largely unjustified assumptions in the case of an extended, strongly driven system), then our model resembles that used in Ref. [6] (i.e. Eq. (4) of Ref. [6]). However, our Eq. (2) applies to any number of components and incorporates time-dependence directly. Even though Eq. (4) of Ref. [6] differs slightly in the form of the coupling from ours, we have previously shown (see Refs. [47–50]) in the limit of λ being time-independent, that many variants of Eq. (2) with different couplings in terms of x, y, z components, generate a similar type of coherent collective state as the one in the present paper. Hence the results in this paper should have broad applicability.

Multi-component resonance Our focus here is on near resonant conditions since these are the most favorable for generating large coherences. Hence we assume for the moment that each component i has one multi-electron energy level separation that is approximately the same as one of the possible vibrational energies, and is also approximately the same for all N components. All other electronic excitation and vibrational modes will be off resonance: including them would modify the quantitative values in our results in Figs. 2–3 but the main qualitative findings would remain. Figures 1(a) and 1(b) provide a motivation for the components in our model inspired by Ref. [6], and a schematic of the resonant version of our model (Eq. (2)) comprising N dimer pairs, where each has two hybridized excitonic states which are energy-split by ϵ . Figure 1(a) shows the example of a single LHII complex [6] based on one of the prototype dimers ubiquitous in light-harvesting antennae of cyanobacteria, cryptophyte algae and higher plants [6]. Indeed LHII is probably the most ubiquitous light-harvesting complex on the planet. There are three candidate components in each LHII complex as shown in Fig. 1(a). Each comprises two hybridized excitonic states with energy splitting $\epsilon = \sqrt{\Delta^2 + 4V^2}$ where Δ is the energy difference between the two chromophores' individual exciton states and V is the dipole-dipole coupling strength that provides the inter-chromophore coupling and hence hybridization [6]. As noted in Ref. [6], the Chlb_{b-a} pair has a mode around 750cm⁻¹ that is coupled to the electronic dynamics, and this energy is also close to the frequency of the pyrrole in-plane deformations – meaning that if driven anharmonically, it could in principle generate time-dependent couplings $\lambda(t)$ as in Eq. (2). We also note that even this single-mode resonance assumption can be generalized by matching up different excitation energies ϵ' , ϵ'' , etc. to the nearest vibrational energies ω' , ω'' etc. and then solving Eq. (2) in the same way for each subset (ϵ', ω') etc. For example, if the N components are partitioned into n subpopulations, where each subpopulation has the same resonant energy and vibrational mode but where these values differ between subpopulations, the total Hamiltonian will approximately decouple into $H^{(1)} \oplus H^{(2)} \oplus H^{(3)} \dots \oplus H^{(N)}$. Any residual coupling between these subpopulations might then be treated as noise, as discussed later.

Temporal coupling from driving field We now justify the claim that memory effects can arise in the exciton-vibration (XV) dynamics due to the interaction with a (controllable) exterior field, and hence justify the use of a time-dependent $\lambda(t)$. For quantum systems embedded in complex environments, where extra degrees of freedom modulate the interaction between the quantum system of interest and a large reservoir, effective non-Markovian behaviors in the quantum system dynamics arise even though the reservoir itself can be described within a Markovian approximation [51]. In our model, the memory effects are due to the parametric pulsed coupling between the exciton and the vibration modes which is represented by the time-dependent XV coupling. Consequently, although it is true that the phase imprinted by the excitation laser is lost during the first steps of electron-exciton relaxation from the high energy sector to the XV region, this is not a sufficient reason to exclude any coherent-like behavior in the relaxing XV dynamics. Indeed it can be shown that for a wide class of phase-mixed states of the pump modes, results for the signal population can be obtained that are identical to those for a coherent population of those modes. In order to clarify this critical point, we now show that our basic premise is justified for a variety of reasons. According to the extensive literature concerning previous versions of a generic Hamiltonian such as that given by Eq. (1), in the classical limit the system is equivalent to two coupled harmonic oscillators. This information is enough to gain analytical insight into the solution of the resulting quadratic system. The driven system in this limit is described by two coupled harmonic oscillators with a time-dependent coupling frequency. Consequently for this purpose, we will consider a simplified model for the parametric process that contains just 3 boson modes (for the sake of simplicity we describe now the N dimer subsystem in the low excitation limit as an effective boson b mode), as described by the Hamiltonian:

$$\hat{H} = \omega_a \hat{a}^\dagger \hat{a} + \chi (\hat{a}^\dagger \hat{a})^2 + \omega_b \hat{b}^\dagger \hat{b} + \omega_c \hat{c}^\dagger \hat{c} + g (\hat{a}^\dagger \hat{b}^\dagger \hat{c}^2 + \hat{a} \hat{b} \hat{c}^{\dagger 2}) \quad (3)$$

where the operators \hat{a} , \hat{b} and \hat{c} correspond to the vibration, exciton and high energy controllable exciton modes as employed in the general Hamiltonian in Eq. (1). Note that we allow for anharmonic terms of strength χ for the vibration mode. We now consider the effect of the pump state on the dynamics of this simple, but representative, model. In particular, we consider the excitation of high energy electron states, which indirectly feeds (through relaxation process) an effective pump reservoir which follows the applied radiation pulse shape. We assume in Eq. (3) that $(\hat{a}^\dagger \hat{b}^\dagger \hat{c}^2 + \hat{a} \hat{b} \hat{c}^{\dagger 2}) = h(t)(\hat{a}^\dagger \hat{b}^\dagger + \hat{a} \hat{b})$ where $h(t)$ represents the applied pulse shape. It is usually argued that the expectation value $\langle \hat{c}^{\dagger 2} \rangle$ ($\langle \hat{c}^2 \rangle$) is different from zero only if the high energy reservoir states have coherent populations. Since the laser pulse excites electrons at a higher energy, the excess energy might be expected to relax into the exciton region giving rise to a coherent interaction. However this is not necessarily the case: after non-resonant excitation, the phase imprinted by the excitation laser is generally lost. The appearance of a well-defined phase is often regarded as the true characteristic feature of a coherent state. However, a careful analysis of unitary dynamics from mixed states, such as those produced by incoherent relaxation processes, shows that coherent-like behaviors can often be obtained. In order to justify this last claim we compute the time evolution of XV observables under two kind of pump initial states: (i) A pure initial state like $|\Psi\rangle = |0_a\rangle |0_b\rangle |\alpha_c\rangle$, denoting the vacuum state for both XV modes, and a pump coherent state. (ii) A statistical mixed state with no phase information at all, given by a density matrix $\hat{\rho}_P = \int_0^{2\pi} d\theta P(\theta) \hat{\Pi}_P(\theta) |\Psi\rangle \langle \Psi| \hat{\Pi}_P^{-1}(\theta)$, where $\hat{\Pi}_P(\theta) = e^{i\hat{N}\theta}$, with $\hat{N} = \hat{a}^\dagger \hat{a} + \hat{b}^\dagger \hat{b} + \hat{c}^\dagger \hat{c}$, denotes a phase smearing operator, given the fact that it takes a pump coherent state $|\alpha_c\rangle$ to a different phase coherent state $|e^{i\theta}\alpha_c\rangle$, leaving the XV modes in the vacuum state. The function $P(\theta)$ fixes the pump phase smearing effect with $P(\theta) \geq 0$ and $\int_0^{2\pi} d\theta P(\theta) = 1$. Since $[\hat{H}, \hat{N}] = 0$, it follows that the time-evolution operator $\hat{U}(t) = e^{-i\hat{H}t}$ commutes with the phase smearing operator $\hat{\Pi}_P(\theta)$. It is now an easy task to obtain for any XV observable like $\hat{a}^{\dagger k} \hat{a}^l$, the time-evolution as

$$\begin{aligned} \langle \hat{a}^{\dagger k} \hat{a}^l \rangle_P &= \text{Tr} \{ \hat{a}^{\dagger k} \hat{a}^l \hat{\rho}_P(t) \} \\ &= \int_0^{2\pi} d\theta P(\theta) \text{Tr} \{ \hat{U}^{-1}(t) \hat{\Pi}_P^{-1}(\theta) \hat{a}^{\dagger k} \hat{a}^l \hat{\Pi}_P(\theta) \hat{U}(t) |\Psi\rangle \langle \Psi| \} . \end{aligned} \quad (4)$$

Since $\hat{\Pi}_P^{-1}(\theta) \hat{a}^{\dagger k} \hat{\Pi}_P(\theta) = e^{-ik\theta} \hat{a}^{\dagger k}$ and $\hat{\Pi}_P^{-1}(\theta) \hat{a}^l \hat{\Pi}_P(\theta) = e^{il\theta} \hat{a}^l$ it follows that

$$\langle \hat{a}^{\dagger k} \hat{a}^l \rangle_P = \langle \hat{a}^{\dagger k} \hat{a}^l \rangle_0 \int_0^{2\pi} d\theta P(\theta) e^{-i(k-l)\theta} \quad (5)$$

where $\langle \hat{a}^{\dagger k} \hat{a}^l \rangle_0$ corresponds to the initial state with the pump in a coherent state. From Eq. (5) it is evident that the population dynamics of the vibrational subsystem ($k = l = 1$) is fully insensitive to this class of phase smearing in the pump state, $\langle \hat{a}^\dagger \hat{a} \rangle_P = \langle \hat{a}^\dagger \hat{a} \rangle_0$, as well as other vibrational correlations as long as the pump phase smearing probability $P(\theta)$ remains practically constant.

The main physical ingredients of the general, complex XV system as given by Eq. (1) are captured by this simple 3-mode Hamiltonian. Therefore we can conclude that for a wide class of coherent pump-plus-relaxation process conditions, our main results on the non-Markovian evolution of the vibrational population are indeed meaningful. Hence the replacement of \hat{c} -pump operators by complex numbers – which consequently yields a time-dependent XV coupling strength $\lambda(t)$ – is justified. Also, the range of validity of our assumption is the same as the usual one for the parametric approximation which requires a highly populated coherent state, $|\alpha_c| \gg 1$, and short times, $gt \ll 1$. These conditions are precisely identical to those under which we show our model fits with previous studies of XV coherence generation: high excitation and a rapid relaxation dynamics. Therefore, there is indeed a formal justification for reducing the last terms in Eq. (3) to $gh(t)(\hat{a}^\dagger \hat{b}^\dagger + \hat{a} \hat{b})$ where $h(t)$ represents the applied pulse shape – hence justifying the time-dependent interaction $\lambda(t) \sim gh(t)$ in Eq. (2).

RESULTS

With a single resonance across all N components in Eq. (2), and all N components having the same resonant excitation energy, the entire $2^{\otimes N} \otimes \mathbb{N}$ dimensional Hamiltonian reduces down to $SU(2)$ collective operators $J_\alpha = \frac{1}{2} \sum_{i=1}^N \sigma_\alpha^i$ where we now drop all the unnecessary component indices. Equation (2) then reduces exactly to $\hat{H} = \epsilon J_z + \omega a^\dagger a + \frac{2\lambda(t)}{\sqrt{N}} J_x (a^\dagger + a)$. For a completely *static* coupling λ and in the limit $N \rightarrow \infty$, there is an electronic-vibrational system phase-boundary at $\lambda_c = \frac{\sqrt{\epsilon\omega}}{2}$. For time-dependent coupling $\lambda(t)$ and finite system size N , this ideal phase transition is not achieved – however the remnant of it is what generates the new forms of collective quantum coherence and non-classicality presented in Figs. 2 and 3 respectively.

Speed drives multi-component quantum coherence Since we are interested in the system's quantum coherences and non-classicality following pulsed perturbations, we take $\lambda(t)$ to be a piecewise linear ramping up and down for simplicity, i.e. triangular profile with total round-trip time τ which acts as an inverse annealing velocity (ramping velocity) v and for the single resonant condition $\epsilon = \omega = 1$. The precise details of $\lambda(t)$ in any particular experiment will depend on the type of nonlinearities induced by the particular probing method, but similar qualitative features to Figs. 2-3 will appear for any up-and-down form. We consider ramping up to $\lambda(t) \approx 1$ and back, though we stress that similar (but weaker) features will be seen for smaller maximum values. For each time t starting at $t = 0$, we obtain numerically the instantaneous state $|\psi(t)\rangle$. Since we are interested in the *additional* coherence generated by the dynamics, we start at $t = 0$ with $|\psi(0)\rangle = \bigotimes_{i=1}^N |\downarrow\rangle \otimes |n=0\rangle$ where both electronic and vibrational subsystems have zero induced excitations. Again, this can be generalized without changing the main details. The accuracy of our numerical solutions was checked by extending the expansion basis beyond the point of convergence. For general ramping velocity v , the amplitude of being either in the ground or the collected excited states, accumulates a dynamical phase with these channels interfering with each other and hence forming the oscillatory patterns. At low ramping velocities, the near-adiabatic regime has a general tendency to show an increase in memory effects as the cycles get faster. However for a broad range of intermediate ramping velocities (Fig. 2) a new regime emerges which is characterized by large quantum coherence between the vibrational and electronic subsystems. This process is fundamentally a squeezing mechanism in both the electronic and vibrational subsystems, followed by the generation of electronic-vibrational coherence in the form of genuine quantum mechanical entanglement [52–54]. As the annealing velocity is further increased, the system has less and less time to undergo any changes. Figure 2 quantifies this electronic-vibrational quantum coherence generated by the applied pulse in terms of the entanglement as measured by the von Neumann entropy. Given a subsystem A , the von Neumann entropy:

$$S_N = -\text{tr} \{ \rho_A \log(\rho_A) \} , \quad \rho_A = \text{tr}_B \{ |\psi\rangle \langle \psi| \} \quad (6)$$

where B is the complementary subsystem and the total system is in a total state $|\psi\rangle$ that is pure. When the total system is in such a pure state, the entropy of subsystem A is equal to the entropy of its complementary subsystem B , and this quantity S_N is a measure of the entanglement between both subsystems. The natural choice in our system for such a bipartition is where one subsystem is the vibrational mode and the other subsystem is the molecular excitonic subsystem. Since this a closed system (i.e. a pure global quantum state with an unitary evolution), the increase of S_N in each subsystem is synonymous with an interchange of information between the vibrations and molecular components during the cycle, hence providing a more direct thermodynamical interpretation for the memory effects of the cycle.

The collective coherence in Fig. 2 is purely quantum in nature (i.e. entanglement); it involves an arbitrary number N of components ($N \geq 3$); and it is achieved using any up-and-down $\lambda(t)$ and *without* the need to access the strong electron-vibrational coupling limit. This is important in practical terms since strong coupling can be hard to generate and control in a reliable way experimentally. Instead, as illustrated in Fig. 2 for each value of N , we find that the same macroscopic coherence is generated by choosing intermediate ramping velocities and undergoing a return trip, as shown. Moreover the same qualitative result as Fig. 2 holds for any $N \geq 3$ and becomes stronger with N . Hence

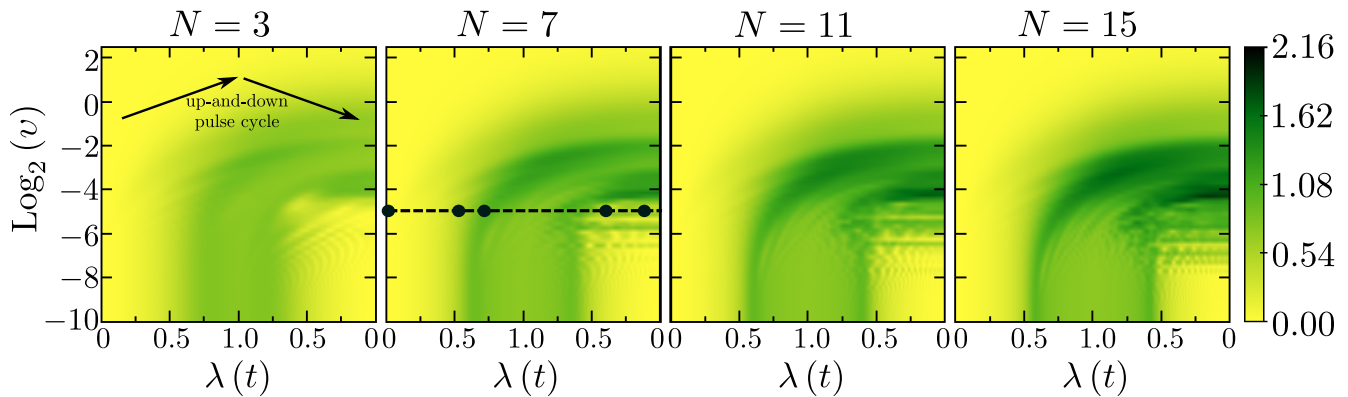


FIG. 2: Collective quantum coherence generated by a simple up-and-down pulse (i.e. triangular $\lambda(t)$ indicated in first panel), as measured by the von Neumann entropy which quantifies the quantum entanglement between the electronic and vibrational subsystems. By the end of just one up-and-down cycle for a broad range of intermediate return trip times, a substantial amount of quantum coherence is generated in the N -component system for general N . If the external perturbation is then turned off, for example because the pulse has ended, the generated coherence will survive as long as the built-in decoherence/dephasing mechanisms in the sample allow it to last. The darker the color, the larger the quantum coherence (see color bar). The larger the v , the less negative the logarithm (i.e. higher on the vertical scale), and the shorter the return trip time. Since these results look qualitatively similar for any $N \geq 3$, they offer insight into the ubiquity of coherences observed empirically in chemical and biophysical systems [1]. Increasing N simply increases the numerical value of the peak value, while choosing a smaller $\lambda(t)$ maximum just reduces the magnitude of the effect. Snapshots of the associated sub-system Wigner functions at the five points along the horizontal dashed line for $N = 7$, are shown in Fig. 3.

we have shown that *by the end of just one up-and-down cycle for a broad range of intermediate return trip times, a substantial amount of quantum coherence will have been generated in the N -component system for general N* . This enhanced XV entanglement region can be seen as bounded by a maximum ramping velocity v_{\max} above which the sudden quench approximation is valid, and a minimum ramping velocity v_{\min} below which the adiabatic condition is fulfilled. v_{\min} does not depend on the maximum value of $\lambda(t)$ reached, which is to be expected since the ground state in the ordered phase has an asymptotic of $S_N \rightarrow \log 2$ and the adiabatic condition should only depend on the system size N . The scaling $v_{\min} \propto N^{-1}$ that emerges, comes from a relation for the minimal energy gap at the critical threshold [52]. The upper bound v_{\max} does not depend on system size. In the near adiabatic regime, the von Neumann entropy is not always increasing with time, which means that for slow annealing velocities, information is not always dispersing from the vibrational subsystem to the molecular subsystem and vice versa. Instead, there is some level of feedback for each subsystem, so that they are still able to retain some of their initial state independence. However, this feedback becomes increasingly imperfect so that at annealing velocities near the boundary with the intermediate regime, the information mixing attains maximal levels. After that, the mixing of information between vibrational and electronic subsystems is always a monotonic dispersion process, which becomes reduced as the time of interaction is reduced more and more. This establishes a striking difference between the lack of memory effects in the adiabatic and sudden quench regimes: the former's cycle comprises a large but reversible change, while the latter's cycle is akin to a very small but irreversible one. In practice, both mean relatively small changes to the initial condition – however this is a consequence of two very different properties. This interplay between actual change and its reversibility may explain why the transition between those two regimes is more intricate than might have otherwise been imagined.

Multi-component non-classicality Our system shows the novel feature of demonstrating non-classicality in both the vibrational *and* the electronic subsystems for arbitrary N , and hence goes well beyond previous analysis restricted to $N = 1$ [6]. Specifically, Fig. 3 shows this non-classicality generated separately within each subsystem during the up-and-down $\lambda(t)$ cycle, and is represented by the AWF (Agarwal-Wigner-Function) and Wigner quasi-distributions for the electronic and vibrational subsystems respectively. As $\lambda(t)$ increases from zero, the Wigner function exhibits squeezing, with the Wigner function then splitting along the x and $-x$ directions and no longer concentrated around the initial state. Increasing $\lambda(t)$ further leads to appearance of negative scars (see red portions) which are uniquely non-classical phenomena – though we stress that even positive portions of W_q and W_b can exhibit quantum mechanical character. Both W_q and W_b not only develop multiple negative regions which are a marker of non-classical behavior, but they also contain so-called sub-Planckian structures which have been related to quantum chaos. Most

importantly, by the end of just one up-and-down cycle, both W_q and W_b have developed complex non-classical patterns, with a blend of regular and chaotic character. Despite being a single vibrational mode, the vibrational field acts as a reservoir that dissipates the quantum correlations present in the squeezed states of each subsystem. If the electronic subsystem were not coupled to the field, squeezing could have revivals after its sudden death.

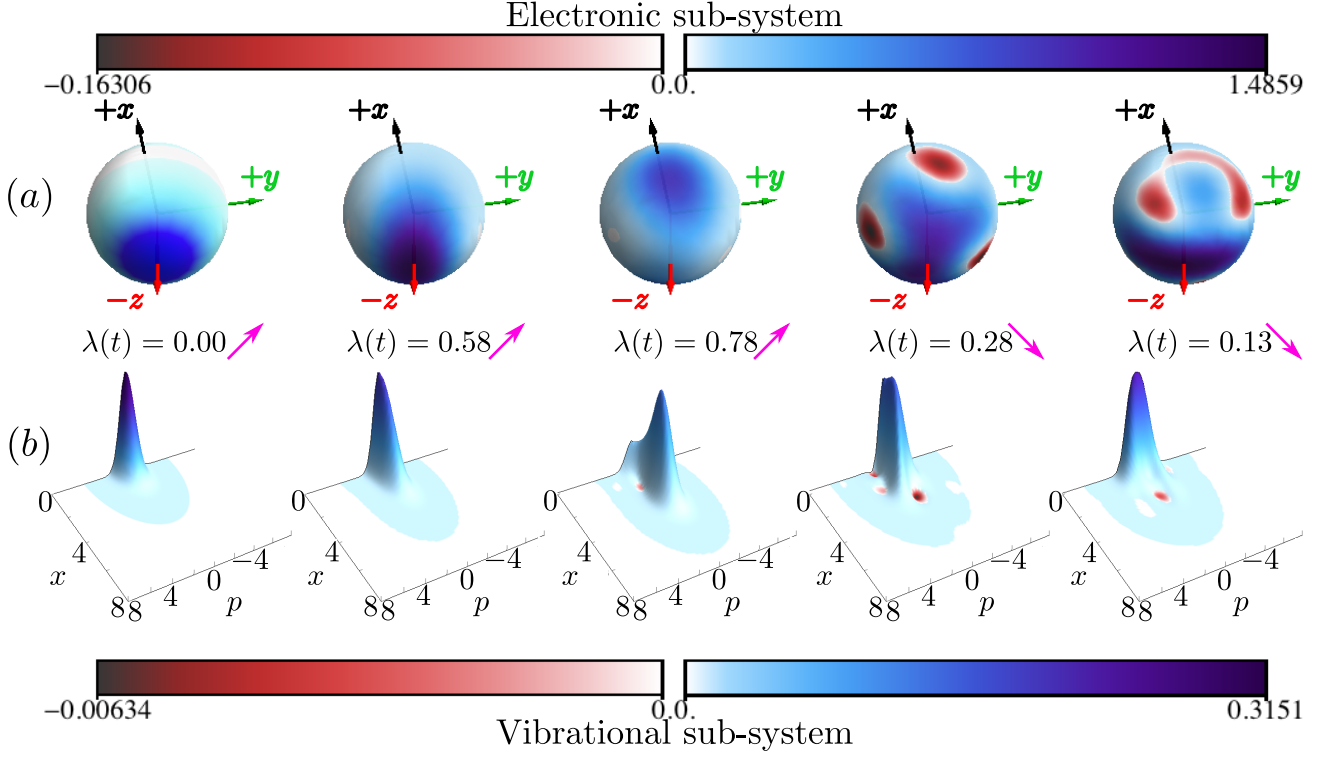


FIG. 3: (a) Electronic sub-system Agarwal-Wigner Functions W_q and (b) vibrational sub-system Wigner functions W_b , shown at two values of $\lambda(t)$ in each portion of an up-and-down pulse cycle. The pulse cycle is the horizontal dashed line in Fig. 2 for $N = 7$. The v value is purposely chosen not to be the optimal one producing the strongest coherence, because we want to illustrate the type of non-classicality that can be achieved for broader values of v . Most importantly, by the end of just one up-and-down cycle, both W_q and W_b develop complex non-classical patterns for a broad range of intermediate return trip times and general $N \geq 3$ (see Fig. 2). W_q and W_b are phase space representations. Though positive portions may be quantum mechanical or classical, the negative portions (red and black) that appear demonstrate unambiguous non-classicality. In (a), opposite Bloch hemispheres are not shown because of symmetry: $W_q(\theta, \phi + \pi) = W_q(\theta, \phi)$. In (b), W_b is represented in the $x-p$ plane of position (vertical) and momentum (horizontal) quadrature. Negative regions of x are not shown because of symmetry: $W_b(x, p) = W_b(-x, -p)$.

Impact of losses and noise Following the density matrix approach of Ref. [52], we have investigated numerically how the presence of losses to the environment in the chemical or biophysical system will affect the dynamics discussed above. All the main results survive well if the decoherence term through interaction with the environment, is anywhere up two orders of magnitudes lower than the main energy scale. Furthermore, even if dissipation is at values of just an order of magnitude below, spin squeezing effects remain highly robust, with increasing noise resistance with system size. Vibrational field squeezing surprisingly survives to dissipation regimes comparable to the Hamiltonian dynamics itself. On the other hand, detailed features of the chaotic stage (such as order parameter oscillations, negative regions, and sub-Planck structures) are far more sensitive to decoherence. These very sensitive features could be used as tools for measuring very weak forces. In our analysis, we have found that introducing small but finite values of the average number of phonons \bar{n} (such as those typical at the ultra-low temperatures in most experimental realizations) does not change qualitatively the conclusions; it just slightly intensifies the process of decoherence.

We have so far assumed a single ϵ, ω pair are close to each other in energy. In the limit that other pairs are also near resonance but these resonances have very different energies from ϵ, ω , a similar dynamical coherence can develop within each of these subspaces of the full Hamiltonian (Eq. (2)). Each pair will have its own up-and-down return trip time (and hence ramping velocity v) for which the coherence is maximal. Since the full Hamiltonian can then be

written approximately as a sum of these separate subspaces, the full many-body wave function will include a product of the coherent wavefunctions $\Psi_{\epsilon',\omega'}(t)$ for these separate $\{\epsilon',\omega'\}$ subspaces. In the more complex case where several pairs are close together in energy, they will each tend to act as noise for each other. Suppose that the coherence for pair ϵ,ω is described by $\Psi_{\epsilon,\omega}(t)$ and it is perturbed by noise from two pairs $\{\epsilon'',\omega''\}$ and $\{\epsilon''',\omega'''\}$ which happen to be nearby in energy. The fact that they are dynamically generated in the same overall system due to the same incident pulses, means that they will likely represent correlated noise. Such correlated noise from various sources can actually help maintain the coherence of $\Psi_{\epsilon,\omega}(t)$ over time. To show this, consider the following simple example (though we stress that there are an infinite number of other possibilities using other numbers and setups, see Ref. [55]) in which we treat $\Psi_{\epsilon,\omega}(t)$ for the pair ϵ,ω as a two-level system. The two subspaces $\{\epsilon'',\omega''\}$ and $\{\epsilon''',\omega'''\}$ each generate decoherence of $\Psi_{\epsilon,\omega}(t)$ in the form of discrete stochastic phase-damping kicks. Such phase kicks are a purely quantum mechanical mechanism for losing coherence, as opposed to dissipation. The probability distributions of the kicks from these two subspaces are P_A, P_B . In addition, the kicks are such that the kick of $\Psi_{\epsilon,\omega}(t)$, described by the rotation angle θ_2 is correlated to the previous rotation angle (θ_1):

$$\begin{aligned} P_A(\theta_2|\theta_1) &= \begin{cases} \frac{1}{3}[\delta(\theta_2) + \delta(\theta_2 + \frac{\pi}{2}) + \delta(\theta_2 - \frac{\pi}{2})], & \text{if } \theta_1 \in \{-\frac{\pi}{2}, 0, \frac{\pi}{2}\}, \\ \delta(\theta_2), & \text{otherwise} \end{cases} \\ P_B(\theta_2|\theta_1) &= \begin{cases} \frac{1}{3}[\delta(\theta_2 - \epsilon) + \delta(\theta_2 + \frac{3\pi}{4}) + \delta(\theta_2 - \frac{\pi}{4})], & \text{if } \theta_1 \in \{-\frac{3\pi}{4}, \epsilon, \frac{\pi}{4}\} \\ \delta(\theta_2 - \epsilon), & \text{otherwise} \end{cases} \end{aligned} \quad (7)$$

with similar conditions holding for all subsequent pairs θ_i and θ_{i-1} (see Ref. [55] for general discussion). The specific choice of angles may be generalized. The parameter ϵ is small, and its presence just acts as a memory of which probability distribution was selected in the previous step. If P_A represents the only noise-source applied, and assuming the initial angle of rotation is 0 (i.e. $\theta_1 = 0$) then $P_A(\theta_n, \dots, \theta_1) = \prod_{i=2}^n P_A(\theta_i|\theta_{i-1}) = (\frac{1}{3})^{n-1}$. Hence if under the influence of subspace $\{\epsilon'',\omega''\}$ (and hence P_A), the density matrix for $\Psi_{\epsilon,\omega}(t)$ will have off-diagonal elements (which correspond to the decoherence) that decrease by a factor $\frac{1}{3}$ after each phase-kick. Similar arguments hold if P_B is the only noise-source applied to the system and if we assume $\theta_1 = \epsilon$. Combining the two noise-sources (i.e. probability distributions) at random means that the angles of rotation can take on seven values, $\{-\pi/3, -\pi/2, 0, \epsilon, \pi/3, \pi/2, \pi\}$. The decay factor now becomes exactly $2/3$ in the limit of $\epsilon \rightarrow 0$. This means that the *combination* of the noise sources causes a slower decoherence of $\Psi_{\epsilon,\omega}(t)$ than each on their own. Hence it is possible that the quantum coherence of $\Psi_{\epsilon,\omega}(t)$ due to a near resonance of ϵ,ω as studied in detail in this paper (Figs. 2-3) is actually favored by having competing coherence processes in the same system.

DISCUSSION

Our study has of course many limitations: the most obvious perhaps being its lack of specific chemical and biological details and hence the apparent difficulty in saying anything specific about a particular chemical or biophysical system in which coherence has been observed. But just as the physics of critical phenomena has been able to obtain predictions about systems-level behaviors of wide classes of chemically distinct materials near critical points *without* including all these details, so too it is possible that the phenomenon of quantum coherence is also, to a certain degree, detail-independent.

With this in mind, our findings predict that chemical or biophysical systems of arbitrary size and driven by pulses (e.g. due to a high power external light source or some other applied field) can show surprisingly strong quantum coherence and non-classicality without necessarily passing to the strong coupling regime, but instead through its dynamics – in particular, the *speed* of the dynamical changes that are induced. As we show in Fig. 2, the resulting coherence builds up during the up-and-down ramping and is large at the end of it. If this ramping is then turned off, for example because the pulse has ended, the generated coherence will survive as long as the built-in decoherence/dephasing mechanisms in the chemical/biophysical system allow it to last. Our calculations show that it could remain for a significant time if the noise is not too large. Our approach complements existing work in that we avoid the usual type of approximations prevalent in the coherence literature [1] and instead present results that in principle apply to general $N \geq 3$. The Hamiltonian that we consider is purposely simpler and more generic than many studied to date in order that we can focus attention on understanding the conditions under which optimal coherence can be generated and hence become available for functional use. Though we considered the coupling λ to be taken to a relatively modest value (~ 1) and returned, even lower maximum values will give qualitatively similar effects.

What about the functional advantage of such coherence? A functional advantage for $N = 1$ has already been discussed in Ref. [6]: in particular, the exciton energy can be transferred coherently from a pure exciton state in a single dimer component, to a mixed excitonic-vibrational state as shown by the individual components in Fig. 1(a). Given that our results apply in principle to an arbitrary number N of components, and these components may in

principle have significant spatial separations, our results point to a new *systems-level* functional advantage in terms of being able to transfer energy and information coherently throughout the entire N -body collective. In particular, since each component (i.e. dimer in Fig. 1) contributes to an important energy transfer pathway towards exit sites, as discussed in Ref. [6], our finding of emergent quantum coherence underpinned by sub-system non-classicalities, implies a systems-level benefit, as opposed to the local advantage for $N = 1$ [6].

There should also a wider range of interest in these findings beyond chemical and biophysical systems, e.g. aggregates of real or artificial atoms in cavities and superconducting qubits [56, 57], as well as trapped ultra-cold atomic systems [58–60], the collective generation and propagation of entanglement [52, 53, 61–65], the development of spatial and temporal quantum correlations [66, 67], critical universality [46], and finite-size scalability [68–70]. Hence the effects described in this paper may be accessible under current experimental realizations in a broad class of systems of interest to physicists. As a result, our findings should be of interest for quantum control protocols which are in turn of interest in quantum metrology, quantum simulations, quantum computation, and quantum information processing [71–75].

Acknowledgments

N.F.J. is very grateful to He Wang for stimulating discussions. F.J.G-R., F.J.R., and L.Q. acknowledge financial support from Facultad de Ciencias through UniAndes-2015 project *Quantum control of nonequilibrium hybrid systems-Part II*. O.L.A. acknowledges support from NSF-PHY-1521080, JILA-NSF-PFC-1125844, ARO, AFOSR, and MURI-AFOSR. N.F.J. acknowledges partial support from the National Science Foundation (NSF) under grant CNS 1522693 and the Air Force under AFOSR grant FA9550-16-1-0247. The views and conclusions contained herein are solely those of the authors and do not represent official policies or endorsements by any of the entities named in this paper.

-
- [1] G. D. Scholes, G. R. Fleming, L. X. Chen, A. Aspuru-Guzik, A. Buchleitner, D. F. Coker, G. S. Engel, R. van Grondelle, A. Ishizaki, D. M. Jonas, et al., *Nature* **543**, 647 (2017).
 - [2] E. Cassette, R. D. Pensack, B. Mahler, and G. D. Scholes, *Nat. Commun.* **6**, 6086 (2015).
 - [3] Y. Fujihashi, G. R. Fleming, and A. Ishizaki, *J. Chem. Phys.* **142**, 212403 (2015).
 - [4] A. Olaya-Castro, C. F. Lee, F. F. Olsen, and N. F. Johnson, *Phys. Rev. B* **78**, 085115 (2008).
 - [5] A. W. Chin, J. Prior, R. Rosenbach, F. Caycedo-Soler, S. F. Huelga, and M. B. Plenio, *Nat. Phys.* **9**, 113 (2012).
 - [6] E. J. O'Reilly and A. Olaya-Castro, *Nat. Commun.* **5**, 3012 (2014).
 - [7] E. Romero, R. Augulis, V. I. Novoderezhkin, M. Ferretti, J. Thieme, D. Zigmantas, and R. van Grondelle, *Nat. Phys.* **10**, 676 (2014).
 - [8] F. D. Fuller, J. Pan, A. Gelzinis, V. Butkus, S. S. Senlik, D. E. Wilcox, C. F. Yocum, L. Valkunas, D. Abramavicius, and J. P. Ogilvie, *Nat. Chem.* **6**, 706 (2014).
 - [9] H. Yamagata and F. C. Spano, *J. Chem. Phys.* **135**, 054906 (2011).
 - [10] F. C. Spano and H. Yamagata, *J. Phys. Chem. B* **115**, 5133 (2011).
 - [11] F. Dubin, R. Melet, T. Barisien, R. Grousson, L. Legrand, M. Schott, and V. Voliotis, *Nat. Phys.* **2**, 32 (2006).
 - [12] G. D. Scholes, G. R. Fleming, A. Olaya-Castro, and R. van Grondelle, *Nat. Chem.* **3**, 763 (2011).
 - [13] S. John, *Phys. Today* **44**, 32 (1991).
 - [14] G. S. Engel, T. R. Calhoun, E. L. Read, T. Ahn, T. Mancal, Y. Cheng, R. E. Blankenship, and G. R. Fleming, *Nature* **446**, 782 (2007).
 - [15] E. Collini and G. D. Scholes, *Science* **323**, 369 (2009).
 - [16] E. Collini, C. Y. Wong, K. E. Wilk, P. M. G. Curmi, P. Brumer, and G. D. Scholes, *Nature* **463**, 644 (2010).
 - [17] G. Panitchayangkoon, D. Hayes, K. A. Fransted, J. R. Caram, E. Harel, J. Wen, R. E. Blankenship, and G. S. Engel, *Proc. Natl Acad. Sci. USA* **107**, 12766 (2010).
 - [18] H. Wang, L. Valkunas, T. Cao, L. Whittaker-Brooks, and G. Fleming, *J. Phys. Chem. Lett.* **7**, 3284 (2016).
 - [19] C. A. Rozzi, S. Maria Falke, N. Spallanzani, A. Rubio, E. Molinari, D. Brida, M. Maiuri, G. Cerullo, H. Schramm, J. Christoffers, et al., *Nat. Commun.* **4**, 1602 (2013).
 - [20] A. Nitzan and M. A. Ratner, *Science* **300**, 1384 (2003).
 - [21] D. Z. Manrique, C. Huang, M. Baghernejad, X. Zhao, O. A. Al-Owaidi, H. Sadeghi, V. Kaliginedi, W. Hong, M. Gulcur, T. Wandlowski, et al., *Nat. Commun.* **6**, 6389 (2015).
 - [22] P. Rebentrost, M. Mohseni, I. Kassal, S. Lloyd, and A. Aspuru-Guzik, *New J. Phys.* **11**, 033003 (2009).
 - [23] N. Christensson, H. F. Kauffmann, T. Pullerits, and T. Mančal, *J. Phys. Chem. B* **116**, 7449 (2012).
 - [24] V. Tiwari, W. K. Peters, and D. M. Jonas, *Proc. Natl Acad. Sci. USA* **110**, 1203 (2013).
 - [25] M. B. Plenio, J. Almeida, and S. F. Huelga, *J. Chem. Phys.* **139**, 235102 (2013).

- [26] F. Novelli, A. Nazir, G. H. Richards, A. Roozbeh, K. E. Wilk, P. M. G. Curmi, and J. A. Davis, *J. Phys. Chem. Lett.* **6**, 4573 (2015).
- [27] G. D. Scholes and G. Rumbles, *Nat. Mater.* **5**, 683 (2006).
- [28] G. S. Schlau-Cohen, A. Ishizaki, T. R. Calhoun, N. S. Ginsberg, M. Ballottari, R. Bassi, and G. R. Fleming, *Nat. Chem.* **4**, 389 (2012).
- [29] J. L. Brédas, E. H. Sargent, and G. D. Scholes, *Nat. Mater.* **16**, 35 (2016).
- [30] J. Sung, P. Kim, B. Fimmel, F. Würthner, and D. Kim, *Nat. Commun.* **6**, 8646 (2015).
- [31] R. Monshouwer, M. Abrahamsson, F. van Mourik, and R. van Grondelle, *J. Phys. Chem. B* **101**, 7241 (1997).
- [32] G. D. Scholes and G. R. Fleming, *J. Phys. Chem. B* **104**, 1854 (2000).
- [33] A. Ishizaki and G. R. Fleming, *J. Chem. Phys.* **130**, 234111 (2009).
- [34] A. Ishizaki and G. R. Fleming, *Annu. Rev. Condens. Matter Phys.* **3**, 333 (2012).
- [35] A. Chenu and G. D. Scholes, *Annu. Rev. Phys. Chem.* **66**, 69 (2015).
- [36] A. Ishizaki, T. R. Calhoun, G. S. Schlau-Cohen, and G. R. Fleming, *Phys. Chem. Chem. Phys.* **12**, 7319 (2010).
- [37] S. Mukamel, *Annu. Rev. Phys. Chem.* **51**, 691 (2000).
- [38] S. Mukamel, D. Abramavicius, L. Yang, W. Zhuang, I. V. Schweigert, and D. V. Voronine, *Acc. Chem. Res.* **42**, 553 (2009).
- [39] A. Ishizaki and G. R. Fleming, *Proc. Natl Acad. Sci. USA* **106**, 17255 (2009).
- [40] C. Liu, L. Xiang, Y. Zhang, P. Zhang, D. N. Beratan, Y. Li, and N. Tao, *Nat. Chem.* **8**, 941 (2016).
- [41] E. R. Bittner and C. Silva, *Nat. Commun.* **5**, 3119 (2014).
- [42] S. Hoyer, A. Ishizaki, and K. B. Whaley, *Phys. Rev. E* **86**, 041911 (2012).
- [43] S. Rafiq and G. D. Scholes, *J. Phys. Chem. A* **120**, 6792 (2016).
- [44] W. Humphrey, A. Dalke, and K. Schulten, *Journal of Molecular Graphics* **14**, 33 (1996).
- [45] F. J. Rodríguez, L. Quiroga, C. Tejedor, M. D. Martin, L. Vina, and R. Andre, *Phys. Rev. B* **78**, 035312 (2008).
- [46] O. L. Acevedo, L. Quiroga, F. J. Rodríguez, and N. F. Johnson, *Phys. Rev. Lett.* **112**, 030403 (2014).
- [47] C. F. Lee and N. F. Johnson, *Europhysics Letters* **81**, 37004 (2008).
- [48] T. C. Jarrett, C. F. Lee, and N. F. Johnson, *Phys. Rev. B, Rapid Communications* **74**, 121301 (2006).
- [49] C. F. Lee and N. F. Johnson, *Phys. Rev. Lett.* **93**, 083001 (2004).
- [50] T. C. Jarret, A. Olaya-Castro, and N. F. Johnson, *Europhysics Letters* **77**, 34001 (2007).
- [51] A. Budini and H. Schomerus, *Journal of Physics A: Mathematical and General* **38**, 9251 (2005).
- [52] O. L. Acevedo, L. Quiroga, F. J. Rodríguez, and N. F. Johnson, *Phys. Rev. A* **92**, 032330 (2015).
- [53] O. L. Acevedo, L. Quiroga, F. J. Rodríguez, and N. F. Johnson, *New J. Phys.* **17**, 093005 (2015).
- [54] F. J. Gómez-Ruiz, O. L. Acevedo, L. Quiroga, F. J. Rodríguez, and N. F. Johnson, *Entropy* **18**, 319 (2016).
- [55] C. F. Lee, N. F. Johnson, F. Rodríguez, and L. Quiroga, *Fluctuation and Noise Letters* **2**, L293 (2002).
- [56] P. Nataf and C. Ciuti, *Nature Comm.* **1**, 1 (2010).
- [57] O. Viehmann, J. von Delft, and F. Marquardt, *Phys. Rev. Lett.* **107**, 113602 (2011).
- [58] I. Bloch, J. Dalibard, and S. Nascimbène, *Nature Phys.* **8**, 267 (2012).
- [59] C. Schneider, D. Porras, and T. Schaetz, *Rep. Prog. Phys.* **75**, 024401 (2012).
- [60] I. M. Georgescu, S. Ashhab, and F. Nori, *Rev. Mod. Phys.* **86**, 153 (2014).
- [61] A. Osterloh, L. Amico, G. Falci, and R. Fazio, *Nature* **416**, 608 (2002).
- [62] L.-A. Wu, M. S. Sarandy, and D. A. Lidar, *Phys. Rev. Lett.* **93**, 250404 (2004).
- [63] E. Romera and A. Nagy, *Physics Letters A* **375**, 3066 (2011).
- [64] J. Reslen, L. Quiroga, and N. F. Johnson, *Europhys. Lett.* **69**, 8 (2005).
- [65] J. J. Mendoza-Arenas, R. Franco, and J. Silva-Valencia, *Phys. Rev. A* **81**, 062310 (2010).
- [66] Z.-Y. Sun, Y.-Y. Wu, J. Xu, H.-L. Huang, B.-F. Zhan, B. Wang, and C.-B. Duan, *Phys. Rev. A* **89**, 022101 (2014).
- [67] F. J. Gómez-Ruiz, J. J. Mendoza-Arenas, F. J. Rodríguez, C. Tejedor, and L. Quiroga, *Phys. Rev. B* **93**, 035441 (2016).
- [68] J. Vidal and S. Dusuel, *Europhys. Lett.* **74**, 817 (2006).
- [69] O. Castaños, E. Nahmad-Achar, R. López-Peña, and J. G. Hirsch, *Phys. Rev. A* **84**, 013819 (2011).
- [70] O. Castaños, E. Nahmad-Achar, R. López-Peña, and J. G. Hirsch, *Phys. Rev. A* **86**, 023814 (2012).
- [71] R. Schützhold and G. Schaller, *Phys. Rev. A* **74**, 060304 (2006).
- [72] A. M. Rey, L. Jiang, and M. Lukin, *Phys. Rev. A* **76**, 053617 (2007).
- [73] J. Dziarmaga, *Adv. Phys.* **59**, 1063 (2010).
- [74] A. Ü. C. Hardal and Ö. E. Müstecaplıoğlu, *Scientific Reports* **5**, 12953 EP (2015).
- [75] W. Niedenzu, D. Gelbwaser-Klimovsky, and G. Kurizki, *Phys. Rev. E* **92**, 042123 (2015).